THE YOUNG MASSIVE STELLAR CLUSTER SANDAGE-96 AFTER THE EXPLOSION OF SN 2004DJ IN NGC 2403

J. Vinkó[1], K. Sárneczky[1], Z. Balog[2,1], S. Immler[3], B. Sugerman[4], P.J. Brown[5], K. Misselt[2], Gy.M. Szabó[6], Sz. Csizmadia[7], P. Klagyivik[7], M. Kun[7], R. Foley[8], A.V. Filippenko[8], B. Csák[1] and L.L. Kiss[9]

Draft version January 16, 2008

ABSTRACT

The bright supernova 2004dj occured within the young massive stellar cluster Sandage-96 in a spiral arm of NGC 2403, close to other star-forming complexes. New multi-wavelength observations obtained with several ground-based- and space telescopes are combined to study the radiation from Sandage-96 after SN 2004dj faded away. The late-time light curves show that Sandage-96 started to dominate the flux in the optical bands after September, 2006 (+800 days after explosion). The optical fluxes are equal to the pre-explosion ones, suggesting that Sandage-96 has survived the explosion without significant changes in its stellar population. An optical Keck-spectrum obtained at +900 days after explosion shows the dominant blue continuum from the cluster stars shortward of 6000 Å as well as strong SN nebular emission lines redward. The integrated SED of the cluster has been extended into the UV-region by archival *XMM-Newton* and new *Swift* observations, and compared with theoretical models. The outer parts of the cluster have been resolved by *HST* allowing the construction of a color-magnitude diagram. The fitting of the cluster SED with theoretical isochrones results in two possible solutions with ages being 9 ± 1 Myr and 30 ± 10 Myr, depending on the assumed metallicity and the theoretical model family. The isochrone fitting of the color-magnitude diagram indicates that the outer part of the cluster consists of stars having an age dispersion of $16 < t < 63$ Myr, which is similar to that of nearby field stars. This age discrepancy may be resolved by the hypothesis that the outskirt of Sandage-96 is contaminated by stars captured from the field during cluster formation. The young age of Sandage-96 and the comparison of its pre- and post-explosion SEDs suggest a progenitor mass of $15 \leq M_{prog} < 25\ M_{\odot}$.

Subject headings: supernovae: individual (2004dj)

1. INTRODUCTION

The theory of stellar evolution predicts that massive stars ($M \geq 8\ M_{\odot}$) end their life as core-collapse supernovae (CC SNe, e.g. Woosley et al. (2002)). In particular, after the main sequence phase the most massive stars undergo heavy mass loss, become stripped stellar cores and explode as Type Ib/c SNe. Stars close to the lower mass limit of CC are thought to show up as Type II-P SNe. Recent observations to detect the progenitors of CC SNe support this scenario. Currently there are 9 Type II SNe (1987A, 1993J, 1999ev, 2003gd, 2004A, 2004et, 2005cs, 2006my, 2006ov; the latter seven are Type II-P), whose progenitors have been directly identified on pre-explosion frames (see Hendry et al. (2006); Li et al. (2007) and references therein) and their mass estimates resulted in $M \leq 15\ M_{\odot}$ for all of them. Moreover, upper mass limits were derived for a number of other Type II SNe from non-detection of their progenitors (Van Dyk et al. 2003; Maund & Smartt 2005), and the highest upper limit was found as $M \sim 20\ M_{\odot}$. These observations have led to a conclusion that Type II-P SNe likely originate from "low-mass" progenitors with $M \leq 20\ M_{\odot}$ (Li et al. 2006, 2007), and the fate of stars with $M \geq 20\ M_{\odot}$ is probably a Type Ib/c SN explosion.

On the other hand, the progenitors of Type Ib/c SNe (even the brightest/closest ones) have escaped direct detection so far (Crockett et al. 2007a). The most promising candidate is SN 2007gr, which occured in a compact, massive stellar cluster in NGC 1058 that has been detected with *HST* prior to explosion (Crockett et al. 2007b).

SN 2004dj, the closest and one of the brightest SNe after SN 1987A, was a similar, but a Type II-P event. It also occured within a young massive cluster, Sandage-96 in NGC 2403 (Vinkó et al. 2006) (Paper I). SN 2004dj has been extensively studied by multi-wavelength observations (see Paper I for references). In particular, several attempts were made to infer the mass of the progenitor by comparing the pre-explosion magnitudes and colors of Sandage-96 with theoretical SEDs to get the age, hence the turnoff mass, of the cluster. These resulted in a range of possible progenitor masses from $M \sim 12\ M_{\odot}$ to $M \geq 20\ M_{\odot}$ depending on the assumed metallicity and/or reddening (Maíz-Apellániz et al. 2004; Wang et al. 2005; Vinkó et al. 2006). However, all these stud-

Electronic address: vinko@physx.u-szeged.hu
[1] Department of Optics & Quantum Electronics, University of Szeged, Dóm tér 9, Szeged, H-6720 Hungary
[2] Steward Observatory, University of Arizona, Tucson, AZ 85721
[3] Astrophysics Science Division, X-Ray Astrophysical Laboratory Code 662, NASA Goddard Space Flight Center, Greenbelt, MD 20771
[4] Department of Physics and Astronomy, Goucher College, Baltimore, MD 21204
[5] Department of Astronomy and Astrophysics, Penn State University, 525 Davey Laboratory, University Park, PA 16802
[6] Department of Experimental Physics, University of Szeged, Hungary
[7] Konkoly Observatory of Hungarian Academy of Sciences, Budapest, Hungary
[8] Department of Astronomy, University of California, Berkeley, CA 94720-3411
[9] School of Physics, University of Sydney, Sydney, NSW 2006, Australia

ies suffered from the age-reddening and age-metallicity degeneracy (Renzini & Buzzoni 1986), because the available pre-explosion observations covered only the optical and near-IR bands.

The main aim of this paper is to derive further constraints on the progenitor mass of SN 2004dj from post-explosion observations of Sandage-96, made after its re-appearance from the dimming light of the SN. The cluster has been successfully re-detected both from our ground-based and space-based observations, showing no significant change in its light level with respect to the pre-explosion one in the optical. We have extended the wavelength coverage of the observed SED into the UV by new observations with *Swift*/UVOT. Moreover, the cluster has been partially resolved by our new observations with *HST*/*ACS*, which provides an additional opportunity to infer age constraints on its stellar population. We have also made attempts to map the star formation rates (SFRs) and masses of some bright H II complexes in the vicinity of Sandage-96 from narrow-band $H\alpha$-imaging, and compare them with the mass of Sandage-96 which also correlates with the possible cluster age.

The paper is organized as follows. In §2 we present our new multi-wavelength observations made from the ground and space. The SED of the cluster and its color-magnitude diagram is constructed and fitted with theoretical model predictions in §3. We discuss the results in §4 and present our conclusions in §5.

2. OBSERVATIONS

In the followings we describe the multi-wavelength observations of Sandage-96 and SN 2004dj obtained with various instruments.

2.1. *Optical data*

2.1.1. *Ground-based photometry*

The light variation of SN 2004dj in the nebular phase was followed from Konkoly Observatory (see Paper I for the description of the telescopes and detectors). In addition, Johnson-B, Johnson-V and narrow-band $H\alpha$ frames were taken with the 90Prime camera on the 2.3 m Bok-telescope at Steward Observatory, Arizona (Fig. 1, left panel).

The magnitudes of SN 2004dj were calculated via aperture photometry based on the same sequence of local standard stars as in Paper I. The $H\alpha$ frames were treated differently, which is described in §3. The photometric data obtained after May 2005 are summarized in Table 1.

The light curves are plotted in Fig. 2. Following the usual decline in the nebular phase (starting at $\sim$ 100 days after explosion), the light curves approached a constant level around day +800. It is shown in more detail in the right panel of Fig. 2.

The flattening of the light curves, as expected, are due to the increasing contribution of the radiation from Sandage-96, emerging from the fading light of SN 2004dj. In Fig. 2 the dotted horizontal lines mark the pre-explosion magnitudes of Sandage-96 (see Paper I).

From the right panel of Fig. 2 it is visible that the post-explosion magnitudes of Sandage-96 are almost identical with the pre-explosion ones in V, R and I. There is a very slight excess in the $B-$band ($\sim$ 0.1 mag), which is about the same as the photometric uncertainty of the data. Although it cannot be ruled out that this excess is due to some kind of systematic error in the calibration of $B-$band data (the deviation from the pre-explosion level is $\sim 1\sigma$), it is interesting that the ground-based B and V magnitudes agree very well with those obtained by *Swift*/UVOT (see §2.2.2).

2.1.2. *Keck-spectroscopy*

The spectral evolution of SN 2004dj has been followed with the 10 m Keck-telescope (Hawaii). More details of these observations will be published elsewhere. In Fig.3 we present a nebular spectrum made on 23 Dec. 2006, +900 days after explosion. This is clearly a composite spectrum of Sandage-96 and the nebular ejecta of SN 2004dj. Longward of 6000 Å strong emission lines of $H\alpha$, [O I] λ6300, [O I] λ6363 and [Fe II] λ7155 Å, characteristics of a typical nebular Type II-P SN spectrum at late phases, can be identified, Shortward of 6000 Å the blue continuum dominates the spectrum. Na I D appears in emission, which is emerging mostly from the SN ejecta, but $H\beta$ is in absorption. Clearly, the radiation from the young stellar population of Sandage-96 is visible in this regime. The shape of the spectrum is fully consistent with the predictions of population synthesis models (see Paper I and §3).

2.1.3. *HST-observations*

SN 2004dj and its surrounding area was observed with *HST*/*ACS* on Aug.28, 2005, 425 days after explosion (P.I. B. Sugerman). 4 sets of 4 drizzled frames were obtained through the F606W and F814W filters, and 3 sets were recorded with the F435W filter. In the latter case the POLUV polarization filter was also placed into the light beam. This made us possible to study the polarization of the SN light, but slightly complicated the photometry of the F435W frames, causing a systematic shift of the zero-point in the standard transformation (see §3.2).

The *ACS* frames, reduced and calibrated by the *HST* pipeline (including MultiDrizzle), were downloaded from the *HST* archive at Canadian Astronomy Data Centre[10]. Because at the epoch of these observations SN 2004dj was still very bright compared with the rest of Sandage-96, its PSF was subtracted from the *ACS* frames. We have used the TinyTim software[11] (version 6.3) for calculating the *ACS* PSFs in each filter. Since the analytical PSF works less effectively for drizzled frames, the flatfield-corrected *.FLT* frames were used for the PSF-removal. After subpixel registration, the individual frames belonging to the same filter were averaged. The model-PSF was then scaled to the peak of the SN and subtracted from the combined frame.

The result is shown in Fig.4. The encircled region (R = 35 pixel $\sim$ 15 pc) contains Sandage-96 with its unresolved inner and resolved outer parts. Several bright red and blue giants are visible in the outer region. The color of the unresolved inner part is also very blue, in accord with the pre-explosion photometric observations and the proposed young cluster age (see Paper I). It is also visible that SN 2004dj occured near the projected center of the cluster (there are some artifacts due to the incomplete

[10] CADC is operated by the National Research Council of Canada with the support of the Canadian Space Agency.

[11] http://www.stsci.edu/software/tinytim/tinytim.html

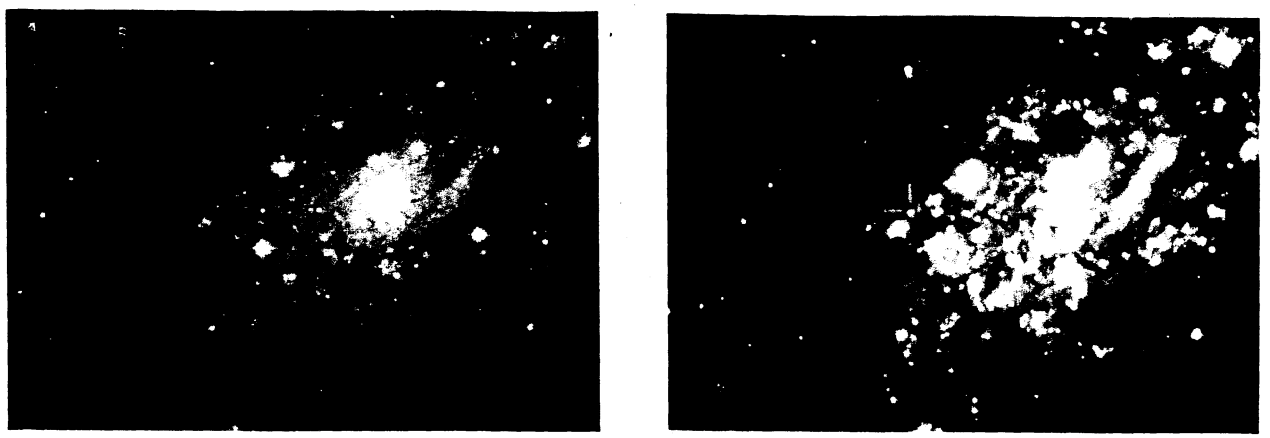

FIG. 1.— Left panel: color-combined B, V and $H\alpha$ frames of NGC 2403 obtained with the 2.3m Bok-telescope at Steward Obs., Arizona on Jan. 28, 2007. Right panel: *Swift*/UVOT image of NGC 2403 obtained on 2 Dec 2007 (U, UVW1 and UVW2 filters were selected as red, green and blue channels). On both panels the position of Sandage-96/SN 2004dj is marked.

TABLE 1
LATE-TINE $BVRI$ PHOTOMETRY OF SN 2004DJ.

Date	JD −2450000	$t - t_{expl}$ (days)	B (mag)	V (mag)	R (mag)	I (mag)	Instrument
2005-11-09	3684.6	500	17.79 (0.08)	17.25 (0.03)	16.69 (0.08)	16.44 (0.06)	Konkoly 0.6m Schmidt
2006-01-27	3762.5	577	17.89 (0.11)	17.68 (0.05)	17.19 (0.11)	16.86 (0.09)	Konkoly 0.6m Schmidt
2006-08-23	3971.6	787	17.93 (0.11)	17.71 (0.05)	17.38 (0.11)	17.00 (0.09)	Konkoly 0.6m Schmidt
2006-09-07	3986.3	801	17.98 (0.07)	17.85 (0.03)	17.50 (0.07)	17.07 (0.06)	Konkoly 1.0m RCC
2006-09-22	4001.6	817	18.22 (0.10)	17.79 (0.04)	17.53 (0.10)	17.08 (0.08)	Konkoly 0.6m Schmidt
2006-10-17	4026.6	842	18.01 (0.09)	17.83 (0.04)	17.53 (0.09)	16.96 (0.08)	Konkoly 0.6m Schmidt
2006-12-22	4092.5	907	18.15 (0.09)	17.88 (0.04)	17.54 (0.09)	17.08 (0.08)	Konkoly 0.6m Schmidt
2006-12-27	4097.6	913	18.11 (0.10)	17.86 (0.04)	17.51 (0.10)	17.08 (0.08)	Konkoly 0.6m Schmidt
2007-01-28	4128.0	943	18.15 (0.06)	17.86 (0.02)	–	–	Steward 2.3m Bok
2007-02-09	4141.4	956	18.13 (0.08)	17.76 (0.04)	17.51 (0.06)	17.01 (0.08)	Konkoly 1.0m RCC
2007-03-06	4166.3	981	18.11 (0.08)	17.87 (0.03)	17.47 (0.06)	16.99 (0.08)	Konkoly 1.0m RCC

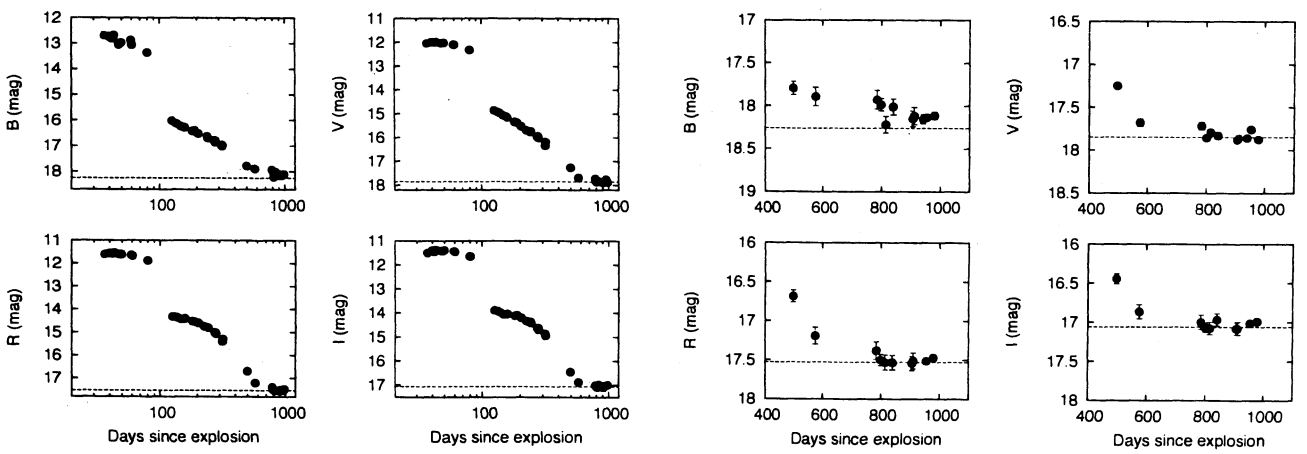

FIG. 2.— $BVRI$ light curves of SN 2004dj from ground-based photometry. The horizontal lines mark the pre-explosion magnitudes of Sandage-96. In the left panel the scaling on the horizontal axis is logarithmic.

PSF-removal at the SN position, but they are less than 1 percent of the subtracted SN flux).

The photometry of the stars appearing on the *ACS* frames has been computed with the DOLPHOT[12] 1.0 software (Dolphin 2000). DOLPHOT incorporates corrections for geometric distortions of the *ACS* camera, cosmic ray removal, object identification, PSF-fitting (using precomputed PSFs via TinyTim), CTE-correction and transformation into standard photometric systems. It works best with the flat-corrected *.FLT* frames. All these frames were processed with DOLPHOT, and the resulting magnitudes belonging to the same filter were combined frame-by-frame. Only those stars that could be identified on at least two frames with the same filter were retained in the final list. The photometric errors were computed from the scattering of the individual data around their mean value, taking into account the individual magnitude errors computed by DOLPHOT. The final magnitudes were converted to Johnson-Cousins B,

[12] http://purcell.as.arizona.edu/dolphot

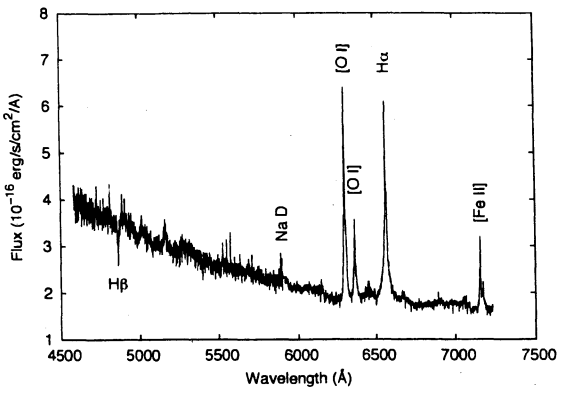

FIG. 3.— Optical spectrum of SN 2004dj/Sandage-96 obtained with the 10 m Keck telescope on Dec. 23, 2006. The identified bright emission lines are formed in the SN ejecta.

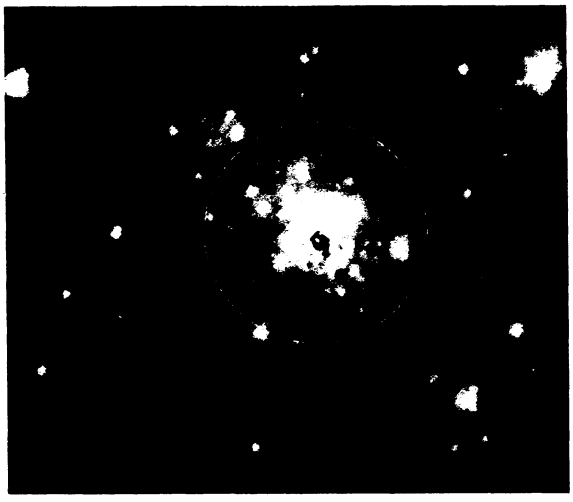

FIG. 4.— Color-combined image of the *HST* F435W (blue), F606W (green) and F814W (red) frames of Sandage-96 obtained on 28 Aug, 2005 (P.I. B. Sugerman). The PSF of SN 2004dj was modeled and removed (see text).

V and I using the calibration by Sirianni et al. (2005). Note that +0.2 mag has been added to the transformed B-magnitudes to take into account the transmission of the *HST* POLUV polarization filter, which was applied together with the $F435W$ filter during the observing run. The results are analyzed in §3.2.

2.2. *UV- and X-ray data*

2.2.1. *XMM-Newton observations*

Prior to the explosion of SN 2004dj, Sandage-96 was observed with the Optical/UV Monitor telescope (OM) aboard *XMM-Newton* (Mason et al. 2001) on 2003-04-30 (P.I.: M. Pakull). The FITS frames and tables containing the photometric data (reduced and calibrated by the SAS-pipeline) were downloaded from the XMM-Newton Science Archive[13]. The instrumental magnitudes of Sandage-96 (object #1057) are listed in Table 2. Unfortunately, no B or V observations were made, thus, full transformation into the standard Johnson-system cannot be computed. However, applying the UV-transformation equations in the OM Calibration Documentation[14], the correction in the U-band is only 0.019 mag, thus, the instrumental magnitudes in Table 2 should represent well the Vega-based standard magnitudes of S96.

Finally, the observed count rates were transformed into fluxes (in erg/s/cm^2/Å) using the conversion factors listed in the OM Calibration Documentation (CAL-TN-0019-3-2, page 17, Table 4). It is known that such a conversion is only approximate, because it depends on the SED of the object. However, the SED of Sandage-96 in the blue/UV regime is very similar to that of an early-type star, or a white dwarf (cf. §3.1). The count-rate-to-flux conversion was calibrated using white dwarf spectrophotometric standards. Therefore, the flux conversion is expected to work fairly well for S96.

2.2.2. *Swift observations*

The *Swift* Observatory (Gehrels et al. 2004) was launched into orbit on Nov. 20, 2004. Its Ultraviolet/Optical Telescope (UVOT, Roming et al. (2005) was used to observe SN 2004dj/Sandage-96 at three epochs. Table 3 summarizes the basic parameters of these observations. A color-combined UV image (made from the data obtained on 2007-12-02) is presented in the right panel of Fig. 1.

The UVOT observations were downloaded from the *Swift* data archive[15]. The sky-subtracted frames were processed and analyzed with a self-developed script in the following way. First, the individual exposures belonging to the same filter (stored as extensions of the same FITS file) were co-added with the UVOTIMSUM routine of the HEAsoft software[16]. Then the summed frames were rebinned by 2 × 2 binning in order to enhance the S/N of the point sources. The fluxes of Sandage-96 and the local photometric standard stars (that could be identified on the UVOT frames) were computed with aperture photometry in *IRAF*. The photometric calibration was done according to the latest prescriptions by Poole et al. (2007). The aperture radius was set as 5 arcsec (5 pixels on the 2 × 2-binned frames), while the sky was computed as the "mode" of the pixel values in an annulus with $r_{in} = 10$ and $r_{out} = 15$ pixels centered on the point source. The summed, sky-corrected fluxes (in ADU) were divided by the dead-time corrected exposure time (defined by the keyword EXPOSURE in the FITS headers) to obtain the raw count rates in ADU s^{-1}. These raw count rates were corrected for coincidence loss following Poole et al. (2007). Finally, the corrected count rates were transformed into magnitudes and physical fluxes in erg·(s cm^{2}Å)$^{-1}$ using the photometric calibrations given by Poole et al. (2007) (note that we have applied the formulae based on the Pickles stellar spectra, instead of the GRB spectra, because the SED of Sandage-96 is more like that of a star than a GRB). No color-term correction was applied to the magnitudes, since we intend to compare physical fluxes rather than magnitudes from UVOT and other instruments. The color-term corrections have been computed only for checking the deviation of the UVOT magnitudes from the magnitudes in the standard Johnson/Bessell system for Sandage-96 (Poole et al. 2007). The corrections are $\Delta U = 0.22$ mag, $\Delta B = 0.03$ mag and $\Delta V = 0.03$ mag, where $\Delta m = m_J - m_{UVOT}$. It is seen that the UVOT B and V magnitudes are fairly

[13] http://xmm.esac.esa.int/xsa/index.shtml
[14] http://xmm.vilspa.esa.es/external/xmm_sw_cal/calib/index.shtml
[15] http://heasarc.gsfc.nasa.gov/cgi-bin/W3Browse/swift.pl
[16] http://heasarc.gsfc.nasa.gov/docs/software/lheasoft/

TABLE 2
XMM-Newton OM OBSERVATIONS OF SANDAGE-96

Obs. ID	Date (UT)	Exp. time (s)	$UVW2$ (mag)	Flux (*)	$UVW1$ (mag)	Flux (*)	U (mag)	Flux (*)
0150651101	2003-04-30	6304	16.87	9.20	16.76	6.59	17.37	4.04
		σ	0.11	0.93	0.06	0.37	0.06	0.23

NOTE. — (*) The fluxes are in 10^{-16} erg/s/cm^2/Å units.

TABLE 3
Swift UVOT OBSERVATIONS OF SN 2004DJ/SANDAGE-96

Obs. ID	Date (UT)	Exp. time (s)	$UVW2$ (mag)	Flux (*)	$UVM2$ (mag)	Flux (*)	$UVW1$ (mag)	Flux (*)	U (mag)	Flux (*)	B (mag)	Flux (*)	V (mag)	Flux (*)
00035870002	2006-10-09	2215	–	–	–	–	16.96	6.98	17.44	3.45	18.02	3.59	17.65	3.24
00035870003	2006-10-15	5553	–	–	–	–	16.91	7.33	17.25	4.08	17.94	3.88	17.81	2.81
00035870004	2007-04-06	2308	16.84	9.61	16.91	6.92	17.00	6.78	17.13	4.58	–	–	–	–
00036563001	2007-12-03	6440	16.81	9.89	16.80	7.66	16.95	7.09	17.31	3.88	18.24	2.93	17.76	2.94
00036563002	2007-12-06	2382	16.99	8.32	17.01	6.31	17.07	6.30	17.24	4.13	18.07	3.44	17.80	2.83
		average	16.88	9.27	16.91	6.96	16.98	6.90	17.27	4.02	18.07	3.46	17.76	2.96
		σ	0.10	0.84	0.11	0.68	0.06	0.39	0.11	0.41	0.13	0.40	0.07	0.20

NOTE. — (*)The fluxes are in 10^{-16} erg/s/cm^2/Å units.

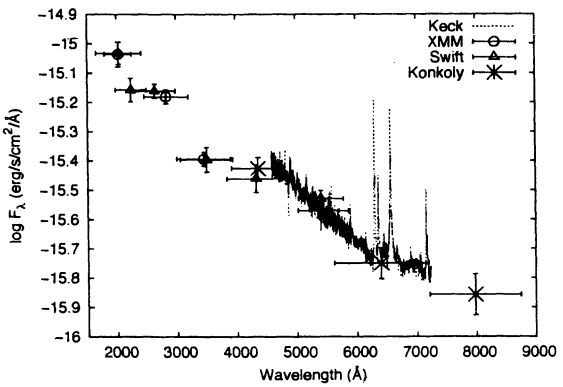

FIG. 5.— Observed SED of Sandage-96 in the UV and optical region. The observatories are indicated as legends. The increase of flux toward shorter wavelengths is continuing in the ultraviolet.

close to the standard system, while the U magnitudes are slightly brighter.

The final UVOT fluxes and their uncertainties are listed in Table 3. They are analyzed further in §3.1.

From our ground-based optical photometry (§2.1) it was concluded that SN 2004dj faded below the light level of S96 in September, 2006 (+800 days after explosion). Because the UV-flux of Type II-P SNe diminishes more rapidly than the optical ones (Immler et al. 2007; Brown et al. 2007), the UVOT observations made in October, 2006 and April, 2007 recorded mostly the cluster light. Fig. 5 shows the comparison of the ultraviolet fluxes with the Keck spectrum (dotted line) and ground-based fluxes (asterisks). The UV fluxes observed by different satellites before and after explosion agree nicely within the errors. The agreement is also very good in the B and V bands, between the ground-based and space-based observations. The differences are ~ 0.06 mag and ~ 0.02 mag in B and V, respectively. A similar agreement was obtained for some of our local photometric standard stars, although most of them were too bright for UVOT.

X-ray data from Stefan can be inserted here !

3. RESULTS

In the followings we present the analysis of the observations outlined in the previous section.

3.1. *SED fitting*

The physical properties of S96 were discussed by Maíz-Apellániz et al. (2004); Wang et al. (2005) and in Paper I. These studies were based on pre-explosion photometry (broad-band Johnson $UBVRI$ and 14-color BATC-system in the optical, and 2MASS JHK in the near-IR) of S96. Fitting the optical and near-IR SED with single stellar population (SSP) models, all these studies revealed that S96 is a young, compact stellar cluster with $\sim 8-20$ Myr age. The age uncertainty is caused by its strong correlation with reddening and metallicity in the SED-fitting, and also its sensitivity to the stellar evolution models applied for constructing the SED of an SSP with a given age.

The SED of young stellar clusters can be best characterized in the UV, because the UV-luminosity, originating from the most massive, fast-evolving supergiants, strongly correlates with the cluster age (O'Connell 1999; Buzzoni et al. 2007). By adding the UV data from *XMM-Newton* and *Swift* (§2.2) to the optical+NIR SED used in the previous studies, there is a good chance to get a better constraint for the cluster age, hence the SN mass.

In Table 4 we have collected all available photometric data (converted to fluxes in erg/s/cm^2/Å) of Sandage-96, including both pre-explosion and post-explosion observations. We have used our $BVRI$ photometry made +800 days after explosion (Table 1) for the representation of the post-explosion flux in the optical. Unfortunately, there are no post-explosion observations in near-IR JHK bands at our disposal. However, in the mid-IR regime the contribution of SN 2004dj is still non-negligible (Sugerman et al., in preparation).

The pre- and post-explosion SEDs are plotted together in Fig. 6. It is apparent that the two datasets agree within the errors. The agreement in the UV- and optical bands implies that the removal of the flux of the progenitor of SN 2004dj from the integrated light of the cluster have not caused a significant loss of light in these bands.

TABLE 4
THE OBSERVED (TIME-AVERAGED) SED OF SANDAGE-96 BEFORE AND AFTER THE EXPLOSION OF SN 2004DJ.

Filter	λ_c	$\Delta\lambda$	F_λ	References
before explosion				
$UVW2_{OM}$	2025	450	9.20 (0.93)	present paper
$UVW1_{OM}$	2825	750	6.59 (0.37)	present paper
a	3360	360	3.11 (0.62)	Wang et al. (2005)
U_{OM}	3450	900	4.04 (0.23)	present paper
U	3663	650	3.58 (0.43)	Larsen (1999)
c	4210	320	3.28 (0.12)	Wang et al. (2005)
B	4361	890	3.33 (0.29)	Paper I
d	4540	340	2.88 (0.08)	Wang et al. (2005)
g'	4872	1280	2.74 (0.10)	Davidge (2007)
e	4925	390	2.54 (0.16)	Wang et al. (2005)
f	5270	340	2.22 (0.10)	Wang et al. (2005)
V	5448	840	2.72 (0.11)	Paper I
g	5795	310	2.18 (0.08)	Wang et al. (2005)
h	6075	310	2.14 (0.11)	Wang et al. (2005)
r'	6282	1150	1.93 (0.10)	Davidge (2007)
R	6407	1580	1.75 (0.15)	Paper I
i	6656	480	1.90 (0.10)	Wang et al. (2005)
j	7057	300	1.98 (0.16)	Wang et al. (2005)
k	7546	330	1.79 (0.09)	Wang et al. (2005)
i'	7776	1230	1.64 (0.10)	Davidge (2007)
I	7980	1540	1.37 (0.17)	Paper I
m	8023	260	1.59 (0.11)	Wang et al. (2005)
n	8480	180	1.50 (0.23)	Wang et al. (2005)
o	9182	260	1.35 (0.13)	Wang et al. (2005)
p	9739	270	1.24 (0.25)	Wang et al. (2005)
J	12200	2130	1.06 (0.08)	Skrutskie et al. (1997)
H	16300	3070	0.70 (0.07)	Skrutskie et al. (1997)
K	21900	3900	0.28 (0.05)	Skrutskie et al. (1997)
after explosion				
$UVW2_{UVOT}$	2030	760	9.27 (0.84)	present paper
$UVM2_{UVOT}$	2231	510	6.96 (0.68)	present paper
$UVW1_{UVOT}$	2634	700	6.90 (0.39)	present paper
U_{UVOT}	3501	875	4.02 (0.41)	present paper
B_{UVOT}	4329	980	3.46 (0.40)	present paper
V_{UVOT}	5402	750	2.96 (0.20)	present paper
B	4361	890	3.75 (0.34)	present paper
V	5448	840	2.69 (0.25)	present paper
R	6407	1580	1.78 (0.23)	present paper
I	7980	1540	1.39 (0.24)	present paper

NOTE. — λ_c and $\Delta\lambda$ denote the central wavelength and the FWHM of a given filter in Å. The fluxes are in 10^{-16} erg/s/cm^2/Åunits. Errors are given in parentheses.

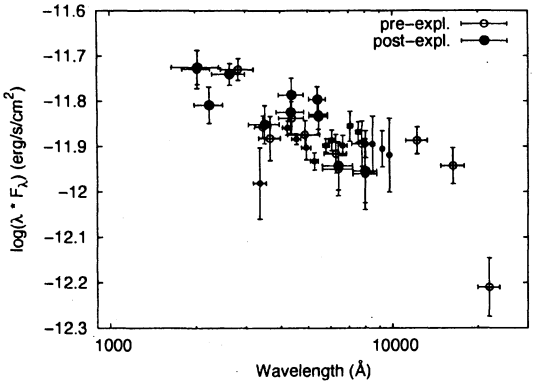

FIG. 6.— Comparison of pre- and post-explosion SEDs of Sandage-96. The two datasets agree within the errors.

In order to fit theoretical SEDs to the observations, we have defined an averaged „normal" SED of S96 by combining the pre- and post-explosion data. In the UV-regime, between 2000 and 4000 Å, we adopted the average of the fluxes from *XMM-Newton*/OM and *Swift*/UVOT. The ground-based data in this spectral regime are expected to be less reliable than the satellite-based ones, because of the higher probability of systematic errors introduced by the local atmospheric conditions. In the optical we used the Johnson-Cousins $BVRI$ data. In the near-IR, only the pre-explosion 2MASS JHK fluxes (Skrutskie et al. 1997) were available for us.

The averaged SED were fitted with theoretical models based on recent stellar evolution calculations. We have applied three different classes of single stellar population (SSP) models with more-or-less different input physics.

First, as in Paper I, we selected the GALAXEV models of Bruzual & Charlot (2003) that are based on the Padova evolutionary tracks. Second, we choose the SPEED models by Jimenez et al. (2004) that were computed using a new set of stellar interior models, evolutionary tracks and different treatment of the mass loss. For both of these models, a Salpeter IMF was adopted, similarly to Paper I and previous studies. The machine-readable data of these two model sets were downloaded from the SPEED website[17].

Third, we applied the SSP models generated by the Starburst99[18] code (Vázquez & Leitherer 2005). The Starburst99 models are highly configurable, the user may choose between different evolutionary tracks, atmospheric models and pre-computed spectral libraries to create a unique set of SSP models. In order to test the model-dependency of the results, we have chosen the Geneva evolutionary tracks, Kroupa IMF, and generated SSP SEDs using $Z = 0.004$, 0.008 and 0.02 metallicities, between $t = 0$ and 100 Myr. Note that the metallicity resolution of the SPEED models is lower, only models with $Z = 0.004$ and 0.02 metallicity are available.

We have fitted the computed SEDs from the above SSP models to the observed „normal" SED described above. During the fitting, the metallicity was kept fixed, and the following parameters were optimized: the cluster mass M_c, the cluster age T_c and the reddening $E(B-V)$. For cluster ages that did not correspond to any pre-computed SSP model, the SED was calculated via interpolation between the closest existing models. The cluster mass was used as a simple scale factor of the model SEDs. Interstellar reddening was parametrized by $E(B-V)$ and $R_V = 3.1$. The interstellar extinction at any wavelength in the considered UVOIR spectral regime was calculated using the averaged galactic reddening law by Fitzpatrick & Massa (2007).

The distance of NGC 2403 was assumed as $D = 3.5$ Mpc. This is found as an optimum by combining various distance measurement results for SN 2004dj and its host galaxy, as discussed in Paper I.

The results of the χ^2-minimization are collected in Table 5 and plotted in Fig 7. These results are basically similar to, and consistent with those from previous calculations (see Paper I). In every case, the solution turned out to be bimodal. It is illustrated in the top-right panel of Fig. 7, where the cluster age and $E(B-V)$ is shown in the x- and y-axis, respectively. There is a deep minimum localized at $T_c = 8$ - 10 Myr, and a similarly deep „valley" between 20 and 40 Myr. These solutions

[17] http://www.astro.princeton.edu/ raulj/SPEED/index.html
[18] http://www.stsci.edu/science/starburst99/

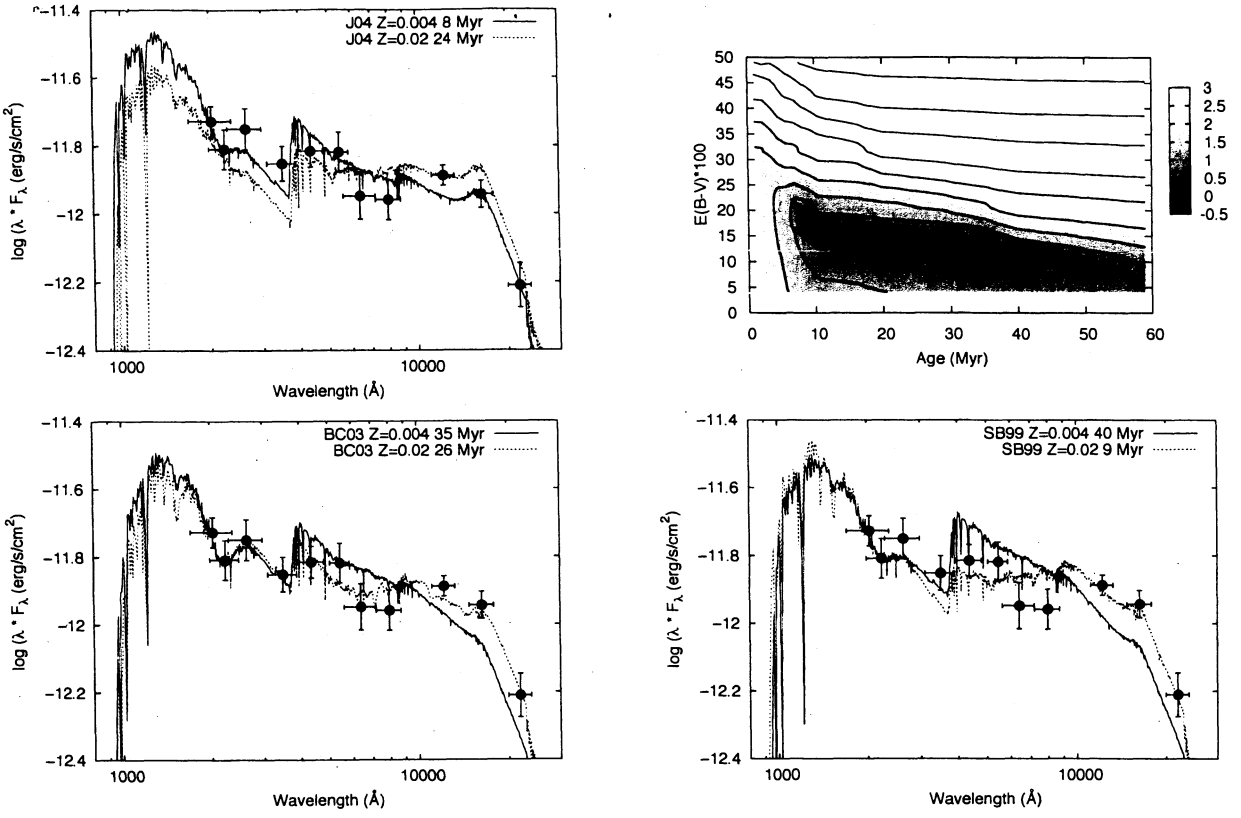

FIG. 7.— SEDs of SSP models fitted to the observations of Sandage-96. Filled circles represent the „normal" SED of the cluster constructed by averaging the observations within the selected wavelength bands (see text). The horizontal errorbars denote the wavelength range of the broadband filters, while the vertical errorbars correspond to the uncertainties of the data. Solid and dotted lines show the theoretical SEDs with parameters indicated as labels. The top-right panel presents the grayscale map of a typical χ^2-space, where the dark areas represent the most probable solutions.

TABLE 5
PARAMETERS OF THE SED FITTING

Model	Z	T_c (10^6 yr)	M_c (10^3 $M_\odot$)	$E(B-V)$ (mag)	χ^2
J04	0.004	8	27	0.09	1.422
J04	0.02	24	99	0.04	2.313
BC03	0.004	35	114	0.13	2.794
BC03	0.02	26	92	0.13	0.536
BC03	0.02	9	37	0.17	0.886
SB99	0.004	40	90	0.08	3.279
SB99	0.008	9	26	0.12	3.521
SB99	0.02	9	24	0.10	1.624

correspond to the „young" and the „old" solutions in Paper I. Clearly, reddening is correlated with age: the „young" solution has generally slightly higher reddening than the „old" solution. Because the χ^2 of these solutions is very similar, it is model dependent which minimum is the deeper one.

Table 5 also illustrates the general correlation between the parameters, known as the „age-metallicity", or „age-reddening-metallicity" degeneracy (Renzini & Buzzoni 1986). However, the correlation is also model-dependent. For the BC03 and SB99 grids, the „old" solution has the lowest χ^2 when the metallicity is sub-solar ($Z = 0.004$), while for $Z = 0.02$ the ages of the best-fitting models are younger. On the other hand, the models by J04 show the opposite: here the low-metallicity best-fitting models are younger.

Contrary to the previous solutions (discussed in Paper I), the reddening parameter is much tighter constrained in this case. It is concentrated around $E(B-V) \sim 0.10 \pm 0.07$, while in the previous studies values as high as $E(B-V) \sim 0.35$ mag were also proposed. The lower reddening is much more consistent with the $E(B-V) = 0.07 \pm 0.1$ mag derived from the observations of SN 2004dj (see Paper I). Although the SED of the whole cluster can, in principle, be much more affected by intracluster reddening than SN 2004dj itself, if the position of the SN within the cluster is on the near side toward the observer, our new *HST*-observations also strongly suggest that $E(B-V) \sim 0.1$ mag for all the stars resolved within the cluster (§3.2). The agreement between these independent constraints for the reddening makes $E(B-V) \sim 0.1 \pm 0.1$ mag very probable.

How can we choose the solution that is the closest one to reality? Breaking the age-metallicity degeneracy needs additional, independent constraints. One possibility is the usage of other metallicity estimates for the host galaxy. Independent observations suggest that the average metallicity of NGC 2403, and in particular Sandage-96, is probably below solar. The oxygen abundance in NGC 2403 at the position of S96 is [O/H] = −0.24, from spectroscopy of H II clouds (Pilyugin et al. 2004). The distribution of red supergiants in the color-magnitude diagram of stars within the inner disk (Davidge 2007) also suggests that the average metallicity of the whole population is $Z \sim 0.008$.

These results may suggest that the solutions with subsolar metallicities are more probable than the ones with $Z = 0.02$. On the other hand, the corresponding cluster

TABLE 6
RESULTS OF THE $H\beta$ FITTING

Z	Track	T_c (10^6 yr)	M_c (10^3 $M_\odot$)	χ^2
0.004	Geneva	9	26	2.470
0.004	Padova	16	65	1.797
0.008	Geneva	9	27	2.355
0.008	Padova	10	40	1.925
0.020	Geneva	10	59	1.413
0.019	Padova	9	44	1.277

NOTE. — $E(B-V)$ was kept fixed at 0.07 mag.

ages are strongly model-dependent. An additional constraint may be the value of the χ^2, although it is sensitive not only to the actual models, but also the estimated uncertainties of the photometric data. Using this criterion, the best-fitting models (with the lowest χ^2 in Table 5) are the BC03 models with solar metallicity. It is interesting that, regardless of metallicity, the solutions with the lowest χ^2 are the „young" ones, but these correspond to different metallicities for different models. This criterion makes the $T_c \sim 9 \pm 1$ Myr solutions more probable.

In the optical, the age of a SSP can be constrained by not only the SED continuum but also the spectral features (Koleva et al. 2008). Comparing the observed features to those of SSP model spectra may give additional constraints on the SSP parameters, such as the age. For young clusters containing several blue supergiants, the Balmer lines are usually the strongest features in the spectrum. We have compared the $H\beta$ line of the high-resolution Keck-spectrum (Sect. 2.1.2) with high-resolution SSP model spectra by Delgado et al. (2005). The fit was computed via χ^2-minimization between 4820 and 4910 Å rest wavelengths. Because the continuum slope was not fitted in this short wavelenght inteval, the reddening parameter was fixed as $E(B-V) = 0.07$ mag (the reddening from SN 2004dj, see Paper I), and only the cluster age and the total cluster mass was optimized. The initial age was restricted to 7 Myr, because of the lack of any visible H II area around Sandage-96 (see §3.3).

The parameters of the best-fitting models are summarized in Table 6. Again, the „young" models produce better fits, regardless of metallicity. The quality of the fit is illustrated in Fig. 8, where the observed spectrum is plotted together with the SSP model spectra against the rest wavelength. In the left panel a 9 and a 35 Myr-old model spectrum (Padova-isochrone, $Z = 0.019$) is compared with the observed $H\beta$ profile. It is apparent that the best-fitting 9 Myr model spectrum fits the wings of the observed line better than the 35 Myr-old one. All other model sequences showed the same behavior. The right panel illustrates the effect of metallicity (showing Geneva models, but the Padova models would be nearly the same). The model with solar metallicity is less deep than the other one with almost the same age, but lower metallicity. The $Z = 0.02$ models are closer to the observed line depths, that is why the χ^2 is the smallest for these models. However, the observed $H\beta$ may contain an emission component from the nebular spectrum of SN 2004dj. This is probable, because $H\alpha$ is entirely dominated by the nebular emission from SN 2004dj (Fig.3). Therefore, the observed $H\beta$ line depth is not a reliable metallicity indicator in this case. Nevertheless, the high-resolution spectral fitting, although with some limitations, favors the „young", i.e. 8 - 10 Myr-old age for Sandage-96.

Finally, we have examined the hypothesis that S96 may not be a SSP resulting from a single, rapid initial starburst. Although a single starburst is a more plausible mechanism for the formation of a massive compact stellar cluster, such as S96, continuous star formation is taking place within the disk of NGC 2403 (Davidge 2007). We have checked if the SED of S96 could be fitted by that of a SSP resulting from continuous star formation rate (SFR). We have computed Starburst99 models with Geneva tracks, Kroupa IMF and different metallicities assuming continuous SFR. The SFR was simply scaled to match the $V-$band observed flux of the cluster SED. Two of the models with $Z = 0.008$ metallicity are plotted in Fig. 9. Regardless of age, these models are too bright in the UV and too faint in the IR, which suggests that the observed SED cannot be described by continuous SFR. The same result has been obtained using other metallicities, or applying the Padova evolutionary tracks, as well.

3.2. *Isochrone fitting*

The computed photometry of the *HST/ACS* frames (§2.1.3) were used to construct color-magnitude diagrams (CMDs) of Sandage-96 using either $B-V$ or $V-I$ as color. We have selected all stars within $R = 35$ pixel (~ 15 pc) around the cluster center (green circle in Fig. 4) as possible cluster members. The visible diameter of the cluster is ~ 15 pixels, corresponding to ~ 6 pc at the distance of NGC 2403.

The CMDs are plotted in Fig. 10, where the filled circles denote the possible cluster members, while crosses represents the other field stars. The number of stars that have $V-I$ color within the cluster region is 34. The field star contamination within this region was estimated by putting an annulus (with the same area as the inner circle) outside the cluster region and counting the stars within this annulus. Using different inner radii for the annulus, but keeping its area fixed, the number of field stars was found to vary between 1 and 5. The number of field stars within the cluster region was therefore estimated as 5 (~ 15 percent).

Fig. 4 also contains the latest Padova isochrones (Cioni et al. 2006a,b) including variable molecular opacities in the TP-AGB phase, with $Z = 0.008$ and $\log t = 6.9$, 7.2 and 7.8, where t is the age in years. The isochrones were reddened with $E(B-V) = 0.07$ mag (§3.1) assuming the galactic reddening law (Fitzpatrick & Massa 2007), and shifted to the 3.5 Mpc distance of the host galaxy. This reddening value seems to be a good estimate for the other field stars as well. The $Z = 0.008$ tracks were selected, because this metallicity is between $Z = 0.004$ and $Z = 0.02$ used in the SED fitting, and these tracks were found the best to describe the distribution of stars on the CMDs. However, very similar results can be obtained by adopting either of these metallicities.

It is apparent that the distribution of the cluster stars on both CMDs cannot be represented by the $\log t = 6.9$ (~ 8 Myr) isochrone. Most of the bright cluster stars lie between the $\log t = 7.2$ (~ 16 Myr) and $\log t = 7.8$ (~ 63 Myr) isochrones, while the fainter ones are located below the latter isochrone. It is also interesting that the field stars follow the same distribution as the cluster members

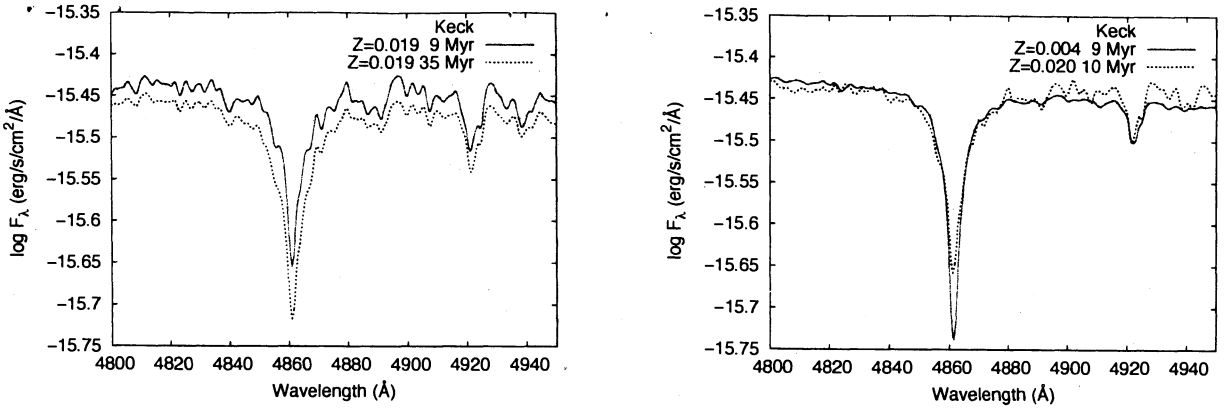

FIG. 8.— The fitting of the observed Keck-spectrum (green dashed curve) with high-resolution SSP models by Delgado et al. (2005). The left panel shows two models based on Padova-isochrones, while the Geneva models are plotted in the right panel. Age and metallicity of the models is indicated in the legend.

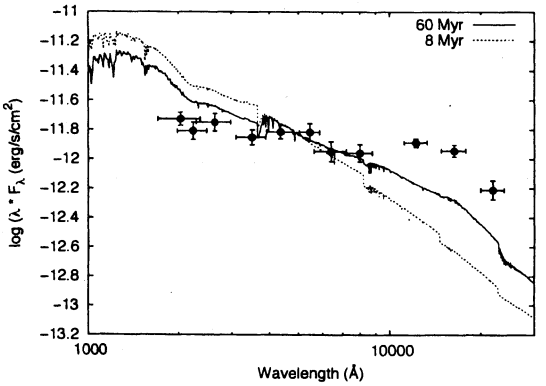

FIG. 9.— Comparison of continuous SFR-models with the observed SED of Sandage-96. The models were generated by the Starburst99 code based on Padova ABG-enhanced tracks with $Z = 0.008$ and Kroupa IMF. The age of the models is indicated as legends. These models (scaled to the average $V-$band flux level) clearly do not fit either the UV- or the IR-flux distribution.

on both CMDs. Note that the blueward distribution of all stars on the V - $(B-V)$ diagram below 23 mag, and the redward distribution on the other CMD below 23.5 mag are due to the decreasing sensitivity of the detector - filter combination in that color regime, i.e. the incomplete detection of objects. The completeness limit was estimated as $V \sim 22.5$ ($M_V \sim -5.2$) mag for the V - $(B-V)$, and $V \sim 23.5$ ($M_V \sim -4.2$) mag for the V - $(V-I)$ diagram.

From Fig. 10 it is concluded that the age of most of the resolved bright cluster stars is between $t \sim 16$ and 63 Myr, which is not significantly different from the age dispersion of the nearby bright field stars. This result contradicts with the age of S96 constrained by the SED fitting ($T_c \sim 8$ - 10 Myr, §3.1). The possible causes of this age-discrepancy is discussed in §4.

3.3. *Star formation rate in the vicinity of S96*

Star formation in NGC 2403 was recently studied by Davidge (2007). From deep *gri* and *JHK* imaging it was found that in the whole disk of NGC 2403 the star formation rate (SFR) during the past 10 Myr has been $\sim 1\ M_\odot\ \mathrm{year}^{-1}$. In addition, the star forming activity was the strongest in the region between 2 - 4 kpc galactocentric distance. This suggests intense star formation activity in the inner disk, which may explain the existence of young, ~ 8 - 10 Myr-old compact clusters, such as S96 ($R_{GC} \sim 2.7$ kpc).

We have examined the SFR of some bright, extended H II areas in the vicinity of S96 to see the value and the variation of the local SFR in this region. For this purpose we used our new narrow-band $H\alpha$ images of NGC 2403 taken with the 2.3-m Bok telescope (see Sect.2 and Table 1). The studied area is shown in Fig. 11. The left panel contains the original $H\alpha$ frame, while the right panel shows the continuum-subtracted one with the considered objects encircled. Five bright H II complexes were selected, three of them (#1, #2 and #3) are within the same spiral arm as S96.

To estimate the continuum level on the $H\alpha$ frame, we have used a scaled V-band frame made with the same telescope and detector. The scaling was done to match the R-band fluxes of the local photometric standard stars (see Paper I) as closely as possible, then the scaled V-frame was subtracted from the observed $H\alpha$ frame. The local photometric standards are dominated by late-type stars, so their R fluxes can be represented with their scaled V fluxes fairly well. As it can be judged from the right panel of Fig. 11, the diffuse background flux due to stellar continuum radiation is much reduced and the contrast between the H II areas and their local background is increased. Thus, most of the fluxes on the residual image in the right panel is likely due to $H\alpha$ emission. Note that there is a significant residual emission at the position of S96, which is expected, because of the bright $H\alpha$ emission coming from the nebular radiation of SN 2004dj (see Fig. 3 and §2.1.2).

In order to determine the $H\alpha$ physical fluxes, we have used the following calibration. We have measured the instrumental fluxes (in ADU) of the local photometric standard stars on the *original*, uncorrected $H\alpha$ frame (left panel in Fig 11), and compared them with their standard R-band fluxes after converting their R magnitudes into fluxes in erg·(s cm^2 Å)$^{-1}$. This resulted in a linear relation, which is plotted in Fig. 12. The fitted line defines the transformation

$$F_\lambda = 10^{-15}[0.75 \cdot 10^{-5} f(H\alpha) - 0.1125], \quad (1)$$

where F_λ is the R-band flux in erg (s cm^2 Å)$^{-1}$ and $f(H\alpha)$ is the observed $H\alpha$ counts in ADU.

We have followed the procedure described by Ramya et al. (2007) for deriving the local SFR of the bright H II areas encircled in Fig. 11. The total observed fluxes of the selected H II areas were computed via aperture

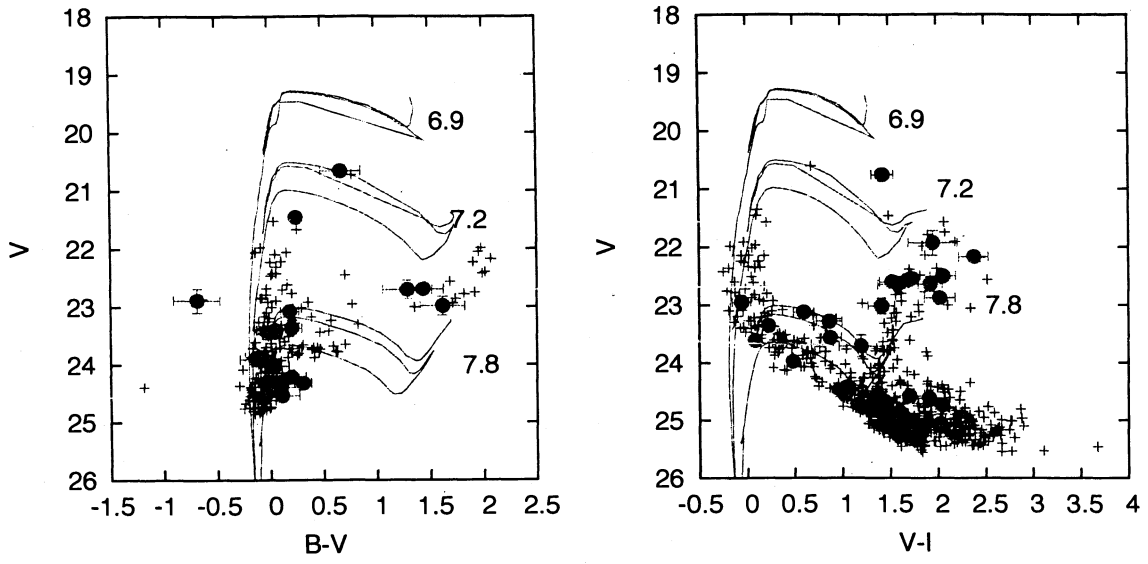

FIG. 10.— *HST* color-magnitude diagrams of Sandage-96 using $B-V$ (left panel), and $V-I$ magnitudes (right panel). Filled circles represent the cluster stars (within the encircled region in Fig.5), while the plus signs denote field stars. The fitted Padova-isochrones of $Z = 0.008$ metallitity are also shown (legends indicate $\log t$, where t is the cluster age in years).

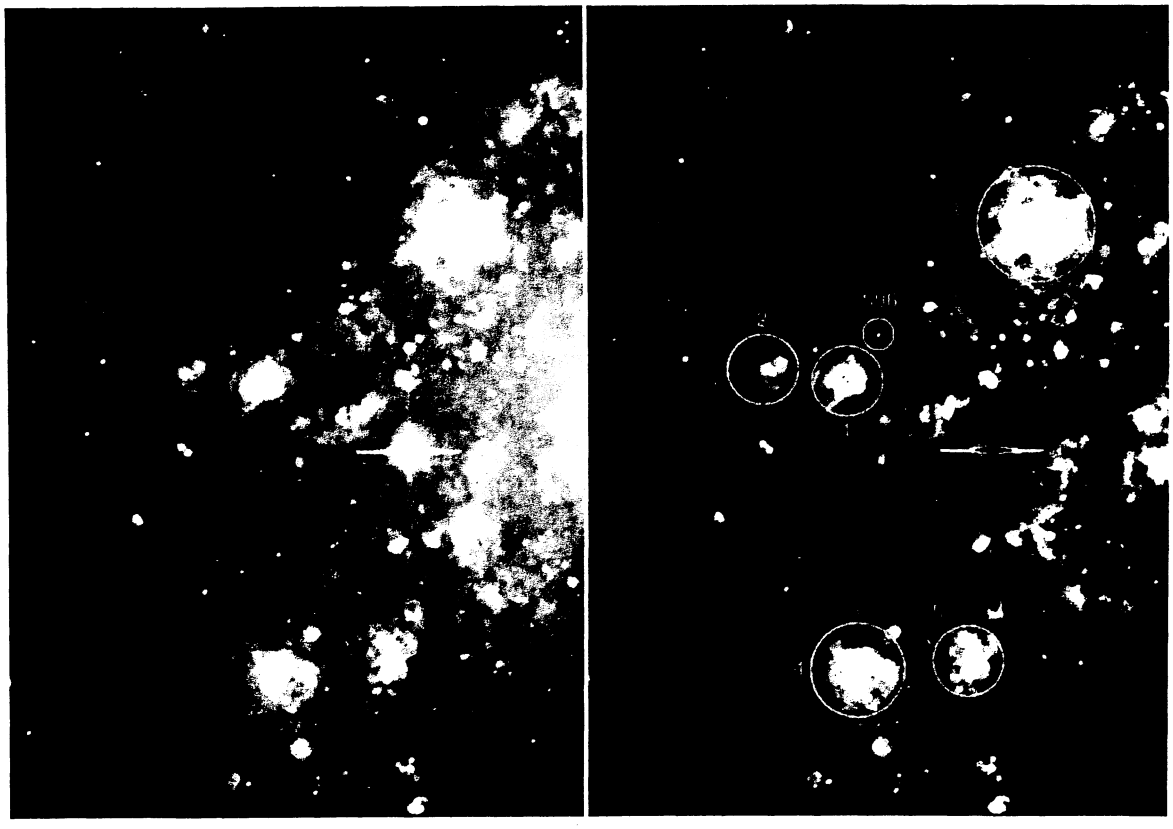

FIG. 11.— Left panel: NGC 2403 in $H\alpha$ filter (from Steward Obs. 2.3m Bok telescope). Right panel: $H\alpha$ image corrected for continuum using scaled V-flux frames.

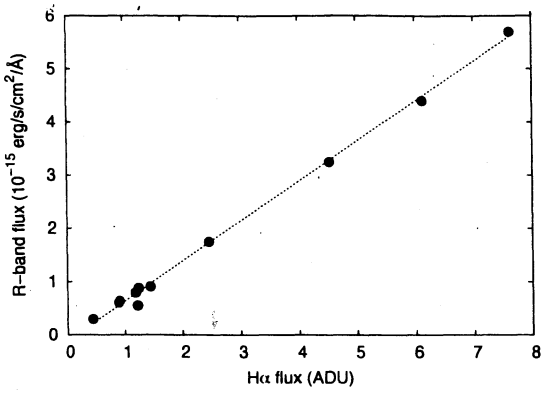

FIG. 12.— Conversion of instrumental $H\alpha$ fluxes into calibrated $R-$band fluxes for field stars around Sandage-96.

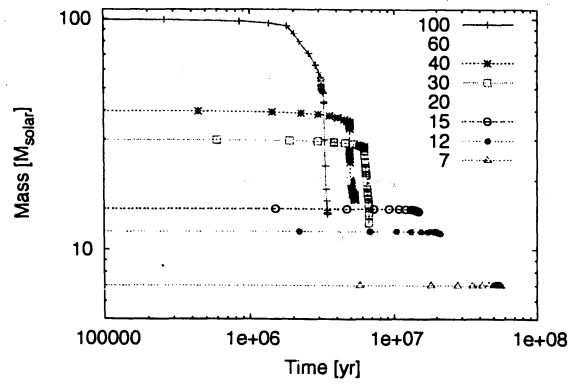

FIG. 13.— Time dependence of masses of stars with $M > 7\ M_\odot$ from Padova tracks. Labels indicate the mass in $M_\odot$.

TABLE 7
SFR OF H II COMPLEXES FROM $H\alpha$-PHOTOMETRY

Id	d	F_λ	log $L(H\alpha)$	SFR	Mass range
	(pc)	(erg/s/cm^2/Å)	(erg/s)	($M_\odot$/yr)	($10^3\ M_\odot$)
1	335	$4.57 \cdot 10^{-15}$	38.83	$5.30 \cdot 10^{-3}$	16 - 37
2	259	$1.16 \cdot 10^{-15}$	38.23	$1.35 \cdot 10^{-3}$	4 - 9
3	548	$4.87 \cdot 10^{-14}$	39.85	$5.64 \cdot 10^{-2}$	169 - 395
4	479	$9.93 \cdot 10^{-15}$	39.16	$1.15 \cdot 10^{-2}$	34 - 80
5	319	$4.27 \cdot 10^{-15}$	38.80	$4.95 \cdot 10^{-3}$	15 - 35

NOTE. — d means the apparent diameter of the complexes in pc, assuming $D = 3.5$ Mpc distance.

photometry on the continuum-subtracted frame. The measured instrumental fluxes were then converted into physical fluxes using Eq.1, and corrected for Milky Way extinction using $A = A_R = 0.107$ mag (taken from NED). It is known that the fluxes from H II regions measured with narrow-band $H\alpha$ filter also contain photons from the [N II] $\lambda\lambda 6548, 6584$ emission lines. Lacking high-resolution spectroscopy of these complexes, we were able to only estimate the contribution of [N II] as ~ 30 % by adopting the mean value of this parameter found by Ramya et al. (2007) for the H II areas in NGC 1084, which also have high SFR like NGC 2403. After removing the [N II] contribution, the resulting $H\alpha$ fluxes were converted into $H\alpha$ luminosities using $D = 3.5$ Mpc for the distance of NGC 2403, then the SFRs were calculated by applying the formula

$$\mathrm{SFR} = 7.9 \cdot 10^{-42}\ L(H\alpha) \qquad (2)$$

(Kennicutt 1998; Pflamm-Altenburg et al. 2007), where SFR is in $M_\odot$ yr^{-1}, and $L(H\alpha)$ is in erg s^{-1}. The results are summarized in Table 7.

Upper and lower limit for the total mass of the stellar contents of these H II areas were also estimated, assuming that the age of the complexes is between 3 and 7 Myr (Ramya et al. 2007). Star forming areas younger than ~ 3 Myr would be deeply buried by molecular clouds preventing their optical detection, while in clusters older than ~ 7 Myr the number of ionising UV photons decrease below the level needed to produce a large ($d \sim 100$ pc) H II cloud (Dopita et al. 2006). The resulting masses are given in the last column of Table 7.

4. DISCUSSION

Comparing the stellar masses of the H II clouds around Sandage-96 (Table 7) with the mass estimates of Sandage-96 given in Table 5, it is apparent that the estimated masses of Sandage-96 are within the stellar mass ranges of the nearby star froming complexes. Moreover, the lack of any extended H II area around S96 implies that it is likely older than the nearby H II complexes, in agreement with its age resulting from SED-fitting (Table 5).

However, the age of Sandage-96 inferred from different techniques appears to be controversial. The SED-fitting (Table 5) resulted in $8 < T_c < 40$ Myr, depending on the assumed metallicity and reddening. The cluster ages derived previously (Maíz-Apellániz et al. 2004; Wang et al. 2005; Vinkó et al. 2006) were distributed between $8 < T_c < 29$ Myr, independent from metallicity, but strongly depending on reddening. In the present study the reddening degeneracy is somewhat reduced, because our observed SED extends well into the UV region, which places strong constrains on the possible reddening and extinction (provided the assumed galactic reddening law is valid for S96). However, the results of the SED-fitting are also strongly model-dependent. Nevertheless, combining all the available constraints from the fitting of the low-dispersion SED and the flux-calibrated high-dispersion spectrum of the cluster (see §3.1) the most probable cluster age seems to be ~ 8 - 10 Myr.

This conclusion is, however, not supported by the fitting of isochrones to the stars appearing in the outer region of S96 resolved by *HST/ACS* (§3.2). From Fig. 10, the possible age of these stars is between $16 < t < 63$ Myr. The average age discrepancy is about a factor of 5 between the different estimates. Note that using isochrones with $Z = 0.02$ metallicity, the same result can be obtained, thus, it seems to be independent from the chosen metallicity (within the considered metallicity range).

How can this age discrepancy be relaxed? The possibility that $T_c > 40$ Myr can be ruled out, because of the significant UV flux in the SED (Fig 7). The most likely hypothesis is the capture of field stars by the massive stellar cluster during its formation, as discussed recently by Pflamm-Altenburg & Kroupa (2007a) for explaining the existence of stars with $t \sim 10$ - 18 Myr within the Orion Nebula cluster, where the bulk of stars have $t < 3$ Myr. The age discrepancy is similar to the case of S96, but otherwise the situation is different, because S96 is much more massive than the Orion Nebula cluster, and the older population resides in the outer region of S96.

Following the argument of Pflamm-Altenburg & Kroupa (2007a), the collapsing pre-cluster cloud may capture nearby field stars during its collapse time, which is roughly equal with its free-fall timescale, $\tau_{ff} \approx (R_c^3/GM_c)^{1/2}$, where R_c is the initial radius of the cloud at the start of the collapse, and M_c is the total mass of the cloud. Adopting $R_c \sim 15$ - 20 pc and $M_c \sim 25$ - 100 $\cdot 10^3$ $M_\odot$, the estimated collapse time of S96 is $\tau_c \sim 2$ - 8 Myr. Note that this is an upper limit for the collapse time, since the mass of the cloud can be significantly higher than the final stellar mass of the cluster (which was used to estimate M_c). Assuming the number density of stars as 2.44 pc^{-3}, Pflamm-Altenburg & Kroupa (2007a) calculated the number of captured field stars within 2.5 pc of the Orion Nebula cluster center as $100 < N < 1000$ if $\tau_c > 2$ Myr. These results suggest that for Sandage-96, which is an order of magnitude more massive than the Orion Nebula cluster, the number of captured field stars should be substantial, even if the number density of the surrounding stars may be lower than that around the Orion cluster. Moreover, we have studied the stellar content within ~ 15 pc from the center of S96, instead of 2.5 pc, which may also increase the number of captured stars. If we interpret the higher age of the stars in the outer part of S96 as a result of field star capture, the photometric data suggest that most of the stars resolved by *ACS* is a captured one, and the young ($t \sim 8$ - 10 Myr), brightest, most massive stars that mostly determine the shape of the integrated SED, reside within the inner ($R \sim 2$ pc), unresolved cluster core. This configuration is roughly consistent with that of other young clusters, as the brightest, massive members are generally found closer to the center.

There might be other mechanisms responsible for the age dispersion within clusters. A possible hypothesis could be a continuous star formation within a $T_c \sim 60$ Myr-old cloud. This scenario can certainly be ruled out, because the SED of such a stellar population is not compatible with the observations (see Fig. 9). Pflamm-Altenburg & Kroupa (2007b) discuss yet another mechanism: gas accretion (and subsequent star formation) from the nearby ISM by a massive cluster. However, according to their simulations, this process is expected to work only for $M_c > 10^6$ $M_\odot$ cluster masses and have a characteristic timescale of a few Gyr. Thus, it is probably unsignificant for S96, for which both the cluster mass and the considered timescale is an order of magnitude less.

The age of Sandage-96 is a key parameter in constraining the mass of the progenitor of SN 2004dj. The classical theoretical limit for the collapse of a stellar core is ~ 8 $M_\odot$, but this can be even 1 - 2 $M_\odot$ smaller depending on the treatment of core convective overshooting (Woosley et al. 2002). This is well supported by recent direct identifications of Type II-P SNe progenitors: their masses determined from observations are between ~ 8 - 15 $M_\odot$ (Maund et al. 2005; Li et al. 2006), none of them exceed $M \sim 20$ $M_\odot$.

If we accept that the progenitor of SN 2004dj is formed together with the bulk of cluster stars within S96, the $M > 8$ $M_\odot$ limit implies $t < 60$ Myr for the cluster according to Padova isochrones. The fact that SN 2004dj occured close to the projected center of Sandage-96 (§2.1.3 and Fig. 4) strongly suggests that its progenitor was indeed a cluster member. Although it was discussed above that Sandage-96 may contain significant number of older stars captured from the field of NGC 2403, it is more probable that a $M > 8$ $M_\odot$ massive star is formed during the collapse of the pre-cluster cloud.

In Fig. 13 the masses of $M > 7$ $M_\odot$ stars are plotted as a function of age from the same Padova evolutionary tracks as above. The final ages of the curves correspond to the last theoretical model for a given initital mass. If we accepted the 8 - 10 Myr age for Sandage-96 inferred from SED-fitting, this would imply $M_{prog} \sim 20$ - 25 $M_\odot$ for the initial mass of the exploding star. Note that the Padova evolutionary tracks do not extend up the actual core collapse, so the final ages for all masses are only lower limits, but an age excess as large as ~ 10 % is hardly expected.

Similarly, if $T_c \sim 30 \pm 10$ Myr was adopted corresponding to the „old" solution of the SED-fitting (and also suggested by the isochrone-fitting, if we disregard the possibility of the presence of captured field stars discussed above), the progenitor mass would be 10 ± 2 $M_\odot$. From fitting the pre-explosion SED, Maíz-Apellániz et al. (2004) and Wang et al. (2005) determined $M_{prog} \sim 12$ - 15 $M_\odot$ depending on the adopted cluster age and reddening. However, their results were more affected by the age-reddening degeneracy (see §3.1), because they had to restrict the wavelength regime of the fitted SED to the optical and near IR due to the lack of observations below 3000 Å. On the other hand, Vinkó et al. (2006) got significantly lower age and higher progenitor mass from nearly the same observed data as Maíz-Apellániz et al. (2004), but using different model SEDs. Therefore, the model-dependency of the cluster age propagates into the mass estimate, adding an additional uncertainty of the derived progenitor mass.

There is yet another possibility to test the possible mass of the progenitor star via the effect of the SN explosion on the integrated cluster SED. The explosion of SN 2004dj must have changed slightly the supergiant population of S96, because one bright (perhaps the brightest) star is missing after the SN faded away. This should be visible in the cluster SED as well, altering both the overall flux level as well as the spectral shape of the post-explosion SED (Maíz-Apellániz et al. 2004). The difference between the pre- and post-explosion SED is approximately the flux spectrum of the progenitor star just before explosion. If the progenitor is a red supergiant (RSG), then mostly the IR regime of the cluster SED will be depressed, while if it is a yellow supergiant (YSG), the change will be more pronounced in the optical.

Fig. 14 shows the comparison of the observed pre- and post-explosion cluster SED with the predictions of this hypothesis. The lines represent the theoretical post-explosion cluster SED if a RSG or a YGS with a given mass is removed from the pre-explosion SED. $M_{prog} =$ 25 $M_\odot$ and 15 $M_\odot$ progenitors were selected for this test, and their parameters were determined from the Padova evolutionary tracks assuming $Z = 0.008$ metallicity.

At first glance, it seems that a 25 $M_\odot$ progenitor can be ruled out, because this model predicts too strong flux decrease in the red part of the cluster SED. The flux decrease is substantial even in the R and I bands. For a 15 $M_\odot$ progenitor, either a RSG or a YSG, the flux

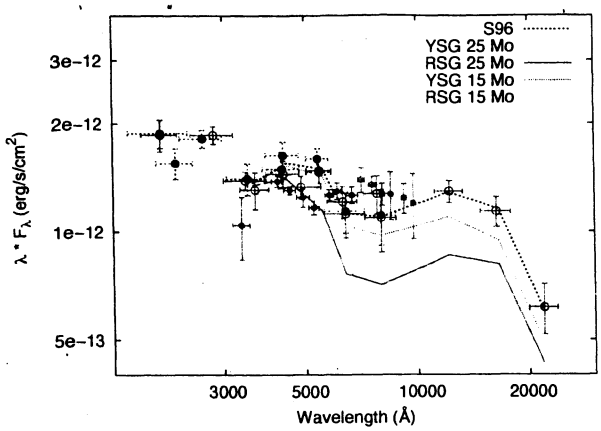

FIG. 14.— The comparison of pre-explosion (red circles) and post-explosion cluster SED data (blue circles). Different lines indicate the change of the SED if the SN explosion destroyed a yellow supergiant (YSG) or a red supergiant (RSG) with a given mass indicated by the labels.

decrease is less, and this model is more consistent with the observations. However, the comparison of the *observed* pre- and post-explosion SEDs of S96 (Fig. 6) also reveals some controversy. First, the proposed *decrease* of the flux has not been observed yet. The pre- and post-explosion fluxes agree within the errors, in the UV and optical bands (cf. §3.1). In the near-IR, we have no post-explosion photometry, but the Keck spectrum indicates that SN 2004dj still makes a non-negligible contribution in the red part of the SED (Fig. 5).

Thus, at present it is doubtful that the observed post-explosion cluster SED can be described as the pre-explosion one minus the spectrum of the SN progenitor. More observations, especially in the near-IR JHK-bands would be very useful to clear this issue. From Fig. 14 it seems that the progenitor mass was probably less than 25 $M_{\odot}$, but it may have been as high as 15 $M_{\odot}$, or even more.

Putting together all available information, it is concluded that the new multi-wavelength observations favor a progenitor star with $15 \leq M_{prog} < 25 M_{\odot}$. This is one of the most massive progenitors of a Type II-P SN determined from observations to date.

5. CONCLUSIONS

We have presented late-time photometry of SN 2004dj and the surrounding cluster Sandage-96, extending the time coverage of the observational sample up to $\sim$ 1000 days after explosion. In the optical, the continuum flux from SN 2004dj faded below the level of the integrated flux of Sandage-96 in Sept., 2006, $\sim$ 800 days after explosion. The pre- and post-explosion SEDs of Sandage-96 show no significant difference between 2000 - 9000 Å. The nebular spectrum of SN 2004dj at $\sim$ 900 days after explosion was dominated by the blue continuum from Sandage-96 shortward of 6000 Å, and strong $H\alpha$, [O I] λ6300, 6363 and [Fe II] λ7155 emission lines, characteristics of a typical nebular spectrum of a Type II-P SN.

We have examined the multi-wavelength observations of Sandage-96 by different methods, in order to get constraints on the cluster age and evolutionary status. The fitting of the cluster SED (using the average of pre- and post-explosion fluxes), resulted in cluster ages between $\sim 9 \pm 1$ and $\sim 30 \pm 10$ Myr. These two solutions appear regardless of the assumed metallicity, but their probability strongly depends on the models used to compute the theoretical SEDs. The range of the possible reddening values is $0.04 < E(B-V) < 0.17$ mag, which is greatly reduced compared with the previous studies, due to the inclusion of the UV-fluxes from *Swift* and *XMM-Newton*.

Sandage-96 appears to be partly resolved on the frames made by *HST/ACS* on Aug.28, 2005 ($\sim$ 425 days after explosion), although the light from SN 2004dj was still very strong at that time. We have computed photometry of the *ACS* frames made through $F435W$, $F606W$ and $F814W$ filters using DOLPHOT, and combined the magnitudes of the detected stellar sources in color-magnitude diagrams. Theoretical isochrones fitted to the observed CMDs revealed that the resolved stars in the outskirts of the cluster have ages between 16 and 63 Myr. The nearby field stars, not associated with S96, show a similar age distribution. This similarity may suggest that most of the cluster stars resolved by *ACS* were captured from the field population during the formation of S96.

From deep $H\alpha$ imaging, star formation rates and possible stellar masses have been estimated for some bright H II clouds in NGC 2403 in the same galactic quadrant where Sandage-96 resides. Sandage-96 is not associated with such a H II region, which is in agreement even with the „young" 9 ± 1 Myr cluster age. The SFRs of the H II complexes are in the order of $\sim 10^{-3}$ - 10^{-2} $M_{\odot}$ yr^{-1}, and their estimated stellar mass is ~ 10 - 100×10^3 $M_{\odot}$, which is similar to the mass range of Sandage-96 found from SED fitting.

The 9 ± 1 Myr age of Sandage-96 would imply a progenitor mass of SN 2004dj as $M_{prog} \geq 20$ $M_{\odot}$, while the 30 ± 10 Myr age would mean $M_{prog} \sim 10$ - 15 $M_{\odot}$, although these estimates are model-dependent. The comparison of the observed pre- and post-explosion cluster SEDs suggests that the light from SN 2004dj may still influences some parts of the cluster SED. Combining all the available pieces of information it is concluded that progenitor had a mass of $15 \leq M_{prog} < 25$ $M_{\odot}$ with the lower limit being more probable. However, more observations, especially in the JHK-bands would be essential to narrow the mass range of the progenitor.

This research has been supported by Hungarian OTKA Grant No. TS049872. The SIMBAD database at CDS, the NASA ADS and NED, and the Canadian Astronomy Data Centre have been used to access data and references. The availability of these services are gratefully acknowledged. **please insert your acknowledgments here!**

REFERENCES

Brown, P. J., et al. 2007, ApJ, 659, 1488
Bruzual, G., & Charlot, S. 2003, MNRAS, 344, 1000
Buzzoni, A., Bertone, E., Chavez, M., & Rodriguez-Merino, L. H. 2007, ArXiv e-prints, 709, arXiv:0709.2711
Cioni, M.-R. L., Girardi, L., Marigo, P., & Habing, H. J. 2006, A&A, 448, 77
Cioni, M.-R. L., Girardi, L., Marigo, P., & Habing, H. J. 2006, A&A, 452, 195

Crockett, R. M., et al. 2007a, MNRAS, 381, 835
Crockett, R. M., et al. 2007b, ArXiv e-prints, 709, arXiv:0709.2354
Davidge, T. J. 2007, ApJ, 664, 820
Delgado, R. M. G., Cerviño, M., Martins, L. P., Leitherer, C., & Hauschildt, P. H. 2005, MNRAS, 357, 945
Dolphin, A. E. 2000, PASP, 112, 1383
Dopita, M. A., et al. 2006, ApJ, 647, 244
Fitzpatrick, E. L., & Massa, D. 2007, ApJ, 663, 320
Gehrels, N., et al. 2004, ApJ, 611, 1005
Hendry, M. A., et al. 2006, MNRAS, 369, 1303
Immler, S., et al. 2007, ApJ, 664, 435
Jimenez, R., MacDonald, J., Dunlop, J. S., Padoan, P., & Peacock, J. A. 2004, MNRAS, 349, 240
Kennicutt, R. C., Jr. 1998, ARA&A, 36, 189
Koleva, M., Prugniel, P., Ocvirk, P., Le Borgne, D., & Soubiran, C. 2008, ArXiv e-prints, 801, arXiv:0801.0871
Larsen, S. S. 1999, A&AS, 139, 393
Li, W., Van Dyk, S. D., Filippenko, A. V., Cuillandre, J.-C., Jha, S., Bloom, J. S., Riess, A. G., & Livio, M. 2006, ApJ, 641, 1060
Li, W., Wang, X., Van Dyk, S. D., Cuillandre, J.-C., Foley, R. J., & Filippenko, A. V. 2007, ApJ, 661, 1013
Maíz-Apellániz, J., Bond, H. E., Siegel, M. H., Lipkin, Y., Maoz, D., Ofek, E. O., & Poznanski, D. 2004, ApJ, 615, L113
Mason, K. O., et al. 2001, A&A, 365, L36
Maund, J. R., & Smartt, S. J. 2005, MNRAS, 360, 288
Maund, J. R., Smartt, S. J., & Danziger, I. J. 2005, MNRAS, 364, L33
O'Connell, R. W. 1999, ARA&A, 37, 603
Pflamm-Altenburg, J., & Kroupa, P. 2007, MNRAS, 375, 855
Pflamm-Altenburg, J., & Kroupa, P. 2007, ArXiv e-prints, 709, arXiv:0709.1943
Pflamm-Altenburg, J., Weidner, C., & Kroupa, P. 2007, ArXiv e-prints, 709, arXiv:0709.1473
Pilyugin, L. S., Vílchez, J. M., & Contini, T. 2004, A&A, 425, 849
Poole, T. S., et al. 2007, ArXiv e-prints, 708, arXiv:0708.2259
Ramya, S., Sahu, D. K., & Prabhu, T. P. 2007, MNRAS, 832
Renzini, A., & Buzzoni, A. 1986, Spectral Evolution of Galaxies, 122, 195
Roming, P. W. A., et al. 2005, Space Science Reviews, 120, 95
Sirianni, M., et al. 2005, PASP, 117, 1049
Skrutskie, M. F., et al. 1997, The Impact of Large Scale Near-IR Sky Surveys, 210, 25
Van Dyk, S. D., Li, W., & Filippenko, A. V. 2003, PASP, 115, 1
Vázquez, G. A., & Leitherer, C. 2005, ApJ, 621, 695
Vinkó, J., et al. 2006, MNRAS, 369, 1780 (Paper I)
Wang, X., Yang, Y., Zhang, T., Ma, J., Zhou, X., Li, W., Lou, Y.-Q., & Li, Z. 2005, ApJ, 626, L89
Woosley, S. E., Heger, A., & Weaver, T. A. 2002, Reviews of Modern Physics, 74, 1015